Journal of Organometallic Chemistry, 192 (1980) 399–408
© Elsevier Sequoia S.A., Lausanne — Printed in The Netherlands

THE BARRIER TO INTERNAL ROTATION IN METALLOCENES

S. CARTER and J.N. MURRELL,
School of Molecular Sciences, University of Sussex, Brighton, BN1 9QJ

(Received December 19th, 1979)

Summary

It has been shown by calculation that the eclipsed forms of ferrocene and ruthenocene are more stable than their staggered forms. The main contribution to the energy difference is the induction energy of the metal in the potential field of the rings. Direct ring—ring electrostatic energy also favours the eclipsed forms by a small amount. The calculated barrier in ferrocene is in good agreement with an experimental estimate from electron diffraction.

---

1. Introduction

Whilst the barriers to internal rotation in biscyclopentadienyl complexes are certainly small there has been some disagreement in the past not only over their magnitude but over whether the eclipsed (D_{5h}) or staggered (D_{5d}) structure is the more stable. The evidence on ferrocene, in particular, has been conflicting.

Early X-ray studies of ferrocene [1—3] suggested a staggered configuration although subsequent work indicated that there might be large rotational oscillations of the rings about their equilibrium position [4]. Rotational disorder was confirmed by neutron diffraction studies [5,6] and the results interpreted by a 1 : 2 population of staggered and eclipsed molecules. In contrast, gas-phase electron diffraction [7,8] gave an eclipsed structure with a barrier to internal rotation of 3.8 ± 1.3 kJ mol^{-1} [8].

There are in fact two crystal structures of ferrocene, a room temperature (RT) and a low temperature (LT) form, and it is the RT form that possesses disorder. The temperature dependence of the NMR signals from the LT form leads to a barrier in the range 7.5—9.6 kJ mol^{-1} [9—11] but the barrier appears to be smaller in the RT form. A new X-ray analysis of the LT form [12] suggests that the molecule has a nearly eclipsed form (a rotation from the exact eclipsed structure by about 10° being indicated) and that the disordered RT form could be described by a statistical distribution of the LT eclipsed structures. A recent neutron diffraction study supports this view [13].

Although the conformation in the crystal is likely to be strongly influenced by crystal forces [14], particularly in view of the fact that heats of sublimation are larger than the barrier to internal rotation, there appears no doubt at this time that the preferred structure of an isolated ferrocene molecule is the eclipsed form.

There have been fewer studies on other biscyclopentadienyl complexes. The X-ray analysis of ruthenocene [14] showed that it had an eclipsed configuration. A number of other metallocenes appear to have a similar crystal disorder to the RT form of ferrocene (see the discussion in ref. 12). Electron diffraction studies of nickelocene and cobaltocene were inconclusive regarding the preferred orientation of the rings but it appears that the barriers to internal rotation are less than in ferrocene [15,16].

Small energy differences can be extremely difficult to explain and the explanation is frequently model dependent. The barrier to internal rotation in ethane and the difference in energy between the FCC and HCP close packed structures of the inert gas solids provide examples of this. We offer in this paper an explanation of the barrier to rotation in ferrocene in the spirit that it is adequate but probably not unique. Our main emphasis is to show an analogy to the situation in the inert gas crystals in that we believe both can be explained on the basis of a non pair-additive induction energy.

In a perturbation theory of long range forces, where the overlap of orbitals on the interacting fragments can be neglected, the induction energy is the only non pair-additive contribution to the energy to second-order of perturbation. For suitable reviews see references 17 and 18. Induction energy is the energy gained by the polarization of an atom or molecule in the combined electrostatic field of all its neighbours.

If overlap cannot be neglected the induction energy can still be defined by the same expressions as in the long range theory but additional non pair-additive terms arise from the exchange of electrons between the fragments [see refs. 17 and 19]. At Van der Waals contacts it is sometimes difficult to decide if the exchange or the overlap independent non-pair energies are the more important. This has been the situation for the inert gas crystals [20].

In a recent paper we have shown that the FCC-HCP energy difference of inert gas crystals can be explained by the induction energy of an atom in the field of its twelve nearest neighbours [21]. In this case the field is non zero because of the small amount of overlap between the orbitals of nearest neighbour atoms. We now propose that the barrier to internal rotation in ferrocene can be explained by the polarization of the metal in the field of the cyclopentadienyl rings. Because the rings undoubtedly carry a net negative charge the induction field is not in this case dependent on overlap for its existence and the induction energy is, in consequence, larger. The parallel between the inert gas and ferrocene problems lies mainly in the fact that the differences between the electrostatic fields for the two structures involved only appear in high orders of spherical harmonics when viewed from the central atom.

Before considering the details of the induction energy we deal briefly with two aspects of direct ring-to-ring interaction in order to show that they are inadequate to explain the barrier.

We first consider the direct overlap of the cyclopentadienyl π orbitals. These transform in D_{5h} symmetry as a_1'', e_1'' and e_2'' in order of increasing energy. In the radical there is an unpaired electron in the e_1'' orbital. Direct overlap of the orbitals of two such radicals would lead to electron pairing and a stabilization which is roughly proportional to the overlap integral.

Using Clementi's 4-term expansion of the carbon $2p$ atomic orbital [22] we calculate the overlap integral between e_1'' orbitals in the eclipsed configuration to be 0.08424, which is perhaps larger than one would expect. However, the difference in overlap integrals between the eclipsed and staggered forms is smaller than this by a factor 5×10^{-3}. Thus to attribute a barrier height of 4 kJ mol^{-1} to this difference would imply an absolute energy from ring-to-ring.overlap of the order of 10^3 kJ mol^{-1} which is unreasonable. At the larger ring-to-ring distance in ruthenocene of 3.7 Å the difference in overlap integrals is even smaller, 3×10^{-4}. We conclude that direct ring-to-ring overlap may make a significant contribution to the total binding energy but not to the barrier.

The rings, being negatively charged, will have a direct ring-to-ring electrostatic repulsion. If we assume that the rings carry unit negative charge and this is distributed 1/5 on each carbon atom then in a point charge approximation the total electrostatic energy of the eclipsed from of ferrocene is 380 kJ mol^{-1} but the difference in energy between the staggered and eclipsed forms is smaller by a factor 10^{-5}.

A more realistic model of the electrostatic energy must take into account the fact that the excess π electron density connat be exactly represented by point charges on the carbon atoms and that the σ electrons will produce their own non-zero potential. We have calculated a complete electrostatic energy assuming a net π electron charge on each ring of 1.125 [23] and a σ electron distribution equivalent to three sp^2 hybrid densities per carbon atom (basis as ref. 22). This calculation predicts that the eclipsed configuration is now more stable than the staggered by 0.53 kJmol^{-1} in the case of ferrocene and 0.09 kJmol^{-1} in the case of ruthenocene. The reason for the change in order from the point charge calculation is that penetration of the π orbitals is more important than the net π charge when this charge is small and penetration favours the eclipsed form.

The dipole—dipole contribution to the dispersion energy between the two rings is invariant to rotation about the C_5 axis. This follows because the (x,y) dipole operators transform as e' in the D_{5h} groups and hence the in-plane dipole polarizability of the rings is axially symmetric. The first multipole polarizability which is not axially symmetric would be of order $l_z = 5$ ($l_z = 1$ for dipole etc.) and the first contribution to the multipole—multipole dispersion which is not axially symmetric is the 5-1 term which would give an energy varying as R^{-14}. Instinct suggests this can be neglected.

2. The induction energy

We will consider only the induction energy arising from the polarization of the central metal ion in the field of the cyclopentadienyl rings. The polarization of a ring in the field of the metal and the other ring will give an axially symmetric energy to high orders of the angular variable. If we adopt a point charge model of the net ring charge as already discussed for the electrostatic energy, then the induction energies will be proportional to the square of the net charge on the ring.

The induction energy is given in second order of perturbation by the expression.

$$E_{\text{ind}} = -\Sigma'_{\text{k}} E_{\text{k}}^{-1} [\int \psi_0 V \psi_{\text{k}} \mathrm{d}v]^2 \tag{1}$$

where ψ_0 is the ground state and ψ_{k} an excited state wavefunction of the metal and V is the electrostatic potential arising from both rings. We follow the procedure used in reference 21 for the inert gas crystals and calculate directly the difference between the induction energies for the eclipsed (e) and staggered (s) forms as follows:

$$(E_{\text{e}} - E_{\text{s}})_{\text{ind}} = -\Sigma'_{\text{k}} E_{\text{k}}^{-1} \int \psi_0 (V_{\text{e}} - V_{\text{s}}) \psi_{\text{k}} \mathrm{d}v \cdot \int \psi_0 (V_{\text{e}} + V_{\text{s}}) \psi_{\text{k}} \mathrm{d}v \tag{2}$$

Let us now suppose that the staggered form is generated from the eclipsed form by rotating the top ring about the z axis by an angle $\phi = 2\pi/10$. Thus $V_{\text{e}} - V_{\text{s}}$ has a non-zero contribution only from the field of the top ring and it has an angular variation which is periodic in $2\pi/5$. It follows that the only states ψ_{k} which give non-zero contributions to expression 2 will be those for which the transition density (3) (N_i is the number of electrons in set i) also has a

$$\rho_{\text{ok}}(1) = N_{\text{i}} \int \psi_0(i) \psi_{\text{k}}(i) \mathrm{d}v_{\text{i} \neq 1} \tag{3}$$

periodicity of $2\pi/5$. Thus if ψ_0 is spherically symmetric ψ_{k} must belong to the set of atomic states $|L,M\rangle$ with $M = \pm 5$ and $L \geqslant 5$.

The contribution to $V_{\text{e}} + V_{\text{s}}$ from the top ring is periodic in $2\pi/10$ and hence it will not contribute to the second integral in expression 2 for states ψ_{k} already selected by the above argument. Thus only the potential of the bottom ring will give a non-zero contribution to this second integral.

Transition densities with odd L and $M = \pm 5$ are symmetric to reflection in the x,y plane and hence for these both integrals in expression 2 have the same sign. Thus states ψ_{k} with odd L stabilize the eclipsed form relative to the staggered; those with even L stabilize the staggered form. $L = 5$ is the leading term and hence we except the induction energy to favour the eclipsed form.

It is possible to use the symmetry of the problem and relate expression 2 to the interaction between the transition density and the field of only one of the carbon atoms in the top layer (which we call atom 1). Expression 2 reduces to

$$(E_{\text{e}} - E_{\text{s}})_{\text{ind}} = (-1)^L 100 \Sigma'_{\text{k}} E_{\text{k}}^{-1} [\int \rho_{\text{ok}}(1) V_1 \mathrm{d}v_1]^2 \tag{4}$$

The factor 100 arises because there are ten equivalent contributions to each integral in expression 2, one from each carbon atom.

Basis states for the calculation have been constructed by exciting electrons from the five highest occupied molecular orbitals of the complex (all doubly occupied), which calculations [23] show to be composed mainly of metal d orbitals, to a set of Slater-type orbitals on the metal.

The calculated d orbital populations are 1.69, 0.7 and 1.62 for d_{z^2}, d_{xz} ($= d_{yz}$) and d_{xy} ($= d_{x^2-y^2}$) respectively [23]. We will assume that all the d orbital population arises from the five highest occupied molecular orbitals and if this is so we deduce that the d orbital coefficients in these molecular orbitals are (ignoring overlap) $(1.69/2)^{1/2}$, $(0.70/2)^{1/2}$ and $(1.62/2)^{1/2}$ respectively. Excitation of one electron from any one of these (ϕ_m) to a vacant orbital (ϕ_n) will give a singlet state and the transition density will be $\sqrt{2}\phi_m\phi_n$. Inserting the appropriate orbital coefficient gives a transition density localized on the metal with weighting factors $1.69^{1/2}$, $0.70^{1/2}$ and $1.62^{1/2}$ for excitation from d_{z^2}, $d_{xz}(d_{yz})$ and $d_{xy}(d_{x^2-y^2})$ respectively.

This localized transition density will in general have several spherical harmonic components but we are only interested in those transforming as $Y_{L\pm5}$. For example, exciting an electron from $d_{z^2}(Y_{20})$ to an orbital transforming as Y_{55} will give a transition density in which the relevant terms are

$$(1.69)^{1/2}\left(-\frac{5\sqrt{5}}{13\sqrt{11}}\left(\frac{11}{4\pi}\right)^{1/2}Y_{55}+\frac{3\sqrt{2}}{13\sqrt{15}}\left(\frac{15}{4\pi}\right)^{1/2}Y_{75}\right)R_{mn}(r) \tag{5}$$

where $R_{mn}(r)$ is the product of the normalized radial wavefunctions of the two metal orbitals involved. This function has to be inserted as $\rho_{\mathrm{ok}}(1)$ in the integral of expression 4. Table 1 gives the relevant terms for the transition densities, for excitations from Y_{20}, $Y_{2\pm1}$ and $Y_{2\pm2}$ into those orbitals which we have found necessary for convergence of expression 4.

Suppose V_1 arises from the carbon atom located at the point $(r_1, \phi_1, 0)$. The integral in expression 4 can be evaluated as in reference 21 by transforming $\rho_{\mathrm{ok}}(1)$ to a new basis of spherical harmonics with the z axis along $(r_1, \theta_1, 0)$ and selecting only the $M = 0$ components in this new basis (V_1 is an axially symmetric potential when viewed along this new z axis). The required components can be obtained from expressions given by Brink and Satchler [24].

Let these $M = 0$ components be donoted by $\mathrm{f}_L(\theta_1)$. Then, for example, the terms in the transition density expression 5 which transform as Y_{55} and Y_{75} about the molecular axis have $M = 0$ components about the new z axis given by

$$\begin{aligned}\mathrm{f}_5(\theta_1) &= (3\sqrt{7}/16)\sin^5\theta\,.\,Y_{50}\\ \mathrm{f}_7(\theta_1) &= (\sqrt{462}/64)\sin^5\theta(13\cos^2\theta-1)Y_{70}\end{aligned} \tag{6}$$

Table 2 lists the values of $\mathrm{f}_L(\theta_1)$ for $\theta_1 = 36.8°$, the angle appropriate to the ferrocene structure.

From expressions 5 and 6 the transition density in expression 4 reduces to

$$\rho_{\mathrm{ok}}(1)=\sum_L \rho^L_{\mathrm{ok}}(1)=\sum_L A_L(\theta_1)Y_{L0}R_{mn}(r) \tag{7}$$

where the constants $A_L(\theta)$ are obtained by multiplying the terms in Table 1 by the appropriate values of $\mathrm{f}_L(\theta_1)$ from Table 2. For example, the transition density (expression 5) becomes

$$\rho_{\mathrm{ok}}(1)=\left(-0.0129\left(\frac{11}{4\pi}\right)^{1/2}Y_{50}+0.0208\left(\frac{15}{4\pi}\right)^{1/2}Y_{70}\right)R_{mn}(r) \tag{8}$$

TABLE 1

THE TRANSITION DENSITIES OF EXPRESSION 5 IN UNITS OF $\left(\frac{2L+1}{4\pi}\right)^{1/2} Y_{L5}R_{mn}(r)$ FOR EXCITATIONS FROM Y_{20}, $Y_{2\pm1}$, $Y_{2\pm2}$

(a) Excitations from Y_{20}

Excited orbital	$L = 5$	6	7	8	9	10	11	12	13	14
$Y_{5\,5}$	−0.3371		0.1096							
$Y_{6\,5}$		−0.1613		0.1451						
$Y_{7\,5}$	0.1280		−0.0645		0.1629					
$Y_{8\,5}$		0.1659		−0.0074		0.1718				
$Y_{9\,5}$			0.1833		0.0280		0.1758			
$Y_{10\,5}$				0.1910		0.0508		0.1769		
$Y_{11\,5}$					0.1933		0.0779		0.1763	
$Y_{12\,5}$						0.1930		0.0758		0.1748

(b) Excitations from $Y_{2\pm1}$

Excited orbital	$L = 5$	6	7	8	9	10	11	12	13
$Y_{4\,4}$		0.1681							
$Y_{5\,4}$	0.1681		0.1821						
$Y_{6\,4}$		0.1626		0.1788					
$Y_{7\,4}$	−0.0366		0.1446		0.1712				
$Y_{8\,4}$		−0.0483		0.1266		0.1628			
$Y_{9\,4}$			−0.0576		0.1109		0.1546		
$Y_{10\,4}$				−0.0635		0.0977		0.1470	
$Y_{11\,4}$					−0.0672		0.0867		0.1401

(c) Excitations from $Y_{2\pm2}$

Excited orbital	$L = 5$	6	7	8	9	10
$Y_{3\,3}$	0.4725					
$Y_{4\,3}$		0.3616				
$Y_{5\,3}$	−0.1205		0.2938			
$Y_{6\,3}$		−0.1505		0.2483		
$Y_{7\,3}$	0.0154		−0.1621		0.2159	
$Y_{8\,3}$		0.0238		−0.1657		0.1918

TABLE 2

THE M = 0 COMPONENTS $f_L(\theta_1)$ OF THE SPHERICAL HARMONICS Y_{L5} IN THE NEW BASIS θ_1 = 36.8°, THE ANGLE APPROPRIATE FOR FERROCENE

f_5	0.030319
f_6	0.101747
f_7	0.190217
f_8	0.285966
f_9	0.361360
f_{10}	0.387608
f_{11}	0.345709
f_{12}	0.235413
f_{13}	0.078368
f_{14}	−0.101402

3. Evaluation of the interaction integrals

Following the procedure given in reference 21, we have chosen transition densities $\rho_{ok}(1)$ which individually maximize the separate contributions to expression 4 of the form

$$E_k^{-1}\left[\int\left(\sum_L A_L(\theta_1)Y_{L0}\right)R_{mn}(r)V_1\mathrm{d}v\right]^2 \tag{9}$$

This was achieved by taking analytical wavefunctions for the occupied d orbitals (ϕ_m) given by Clementi [22] and forming transition densities by exciting an electron to a Slater orbital (ϕ_n) which has the wavefunction

$$\phi_n(\zeta) = \left[\frac{(2\zeta)^{2n+1}}{(2n)!}\right]^{1/2} r^{n-1}\exp(-\zeta r)Y_{lm}(\theta,\phi) \tag{10}$$

where ζ is a variable exponent. For convenience, we write the transition density $\rho_{ok}{}^{L}(1)$ in expressions 7 and 8 in terms of the Roothaan densities [25] which are defined by

$$[NLM] = \left(\frac{2L+1}{4\pi}\right)^{1/2}\frac{2^L(2\bar{\zeta})^{N+2}}{(N+L+1)!}r^{N-1}\exp(-2\bar{\zeta}r)Y_{LM} \tag{11}$$

where $\bar{\zeta}$ is the mean of the exponents of ϕ_m and ϕ_n. The integrals in equation 9 then reduce to expressions such as

$$\frac{(1+\tau)^{m+1/2}(1-\tau)^{n+1/2}}{[(2m)!(2n)!]^{1/2}}\,\frac{(N+L+1)!}{2^L}\int[NL0]V_1\mathrm{d}v_1 \tag{12a}$$

$$\equiv T_{mn}\,\frac{(N+L+1)!}{2^L}\int[NL0]V_1\mathrm{d}v_1 \tag{12b}$$

where m and n denote the principal quantum numbers of ϕ_m and ϕ_n respectively, $N = m + n - 1$ and

$$\tau = \frac{\zeta_m - \zeta_n}{\zeta_m + \zeta_n} \tag{13}$$

These integrals were evaluated by taking the potential V_1 as the potential of a carbon atom already described in section 1, i.e. an effective nuclear charge of +4, one electron in each σ sp^2 hybrid and an amount Q in the $2p\pi$ orbital. It can be shown that this gives rise to the potential

$$V_1 = -\frac{4}{r_1} + T_{ss}[3S] + (2+Q)T_{pp}[3s] +$$
$$+\frac{3}{2}(\cos^2\theta_1.(2Q-1) + \sin^2\theta_1.(2-Q) - 1)T_{pp}[3D\Sigma] \quad (14)$$

where T_{ss} and T_{pp} are equivalent to T_{mn} in expression 12b and indicate that the corresponding transition densities involve electrons in carbon $2s$ and $2p$ orbitals respectively. $[3D\Sigma]$ is shorthand for [320] etc. The integrals were evaluated in part by Roothaan's method [25], the final one-electron integration being carried out numerically [26].

The energy denominator in expression 9 has been calculated assuming that the dependence of this energy on the exponent (ζ) of the upper state orbital ϕ_n is the same as it is for the excitation of a one-electron atom [21]. The orbital energies have the form (in hartrees)

$$E_{N,L} = \frac{\zeta^2}{2} - \frac{\zeta}{N} \quad (15)$$

and if $L = N - 1$

$$E_L = \frac{\zeta^2}{2} - \frac{\zeta}{L+1} \quad (16)$$

For the zero-order energy of the metal d orbitals, we have taken the d orbital energies of the Clementi wavefunction [22] for the atomic ground state.

4. Results

Figures 1 and 2 show the contributions to expression 9, for ferrocene and ruthenocene respectively, from the states constructed by excitation from the occupied d orbitals to a single optimized orbital of quantum number L. Exponent optimization was made independently for each of the three types of d orbital. The metal—carbon distances are 3.836 a_0 for ferrocene and 4.176 a_0 for ruthenocene [4,14].

It is seen that convergence is relatively slow particularly for excitation from Y_{20} and $Y_{2\pm1}$, but has been achieved by $L = 13$. Convergence is primarily due to the magnitude of the integral in expression 9 and not by the factors in Tables 1 and 2 or the excitation energy. However, it should be noted that the factors of Table 1 do become zero as $L \rightarrow \infty$ whereas those in Table 2 do not.

Total stabilization energies are obtained by summing all contributions (contributions from Y_{21} and Y_{22} must be doubled to allow for Y_{2-1} and Y_{2-2}) multiplied by the atomic populations 1.69, 0.70 and 1.62 for Y_{20}, $Y_{2\pm1}$ and $Y_{2\pm2}$ respectively. The final result is a stabilization of the eclipsed form relative to the staggered by 2.25 kJ mol^{-1} in the case of ferrocene and 4.57 kJmol^{-1} for ruthenocene. The induction energy is greater for ruthenocene even though

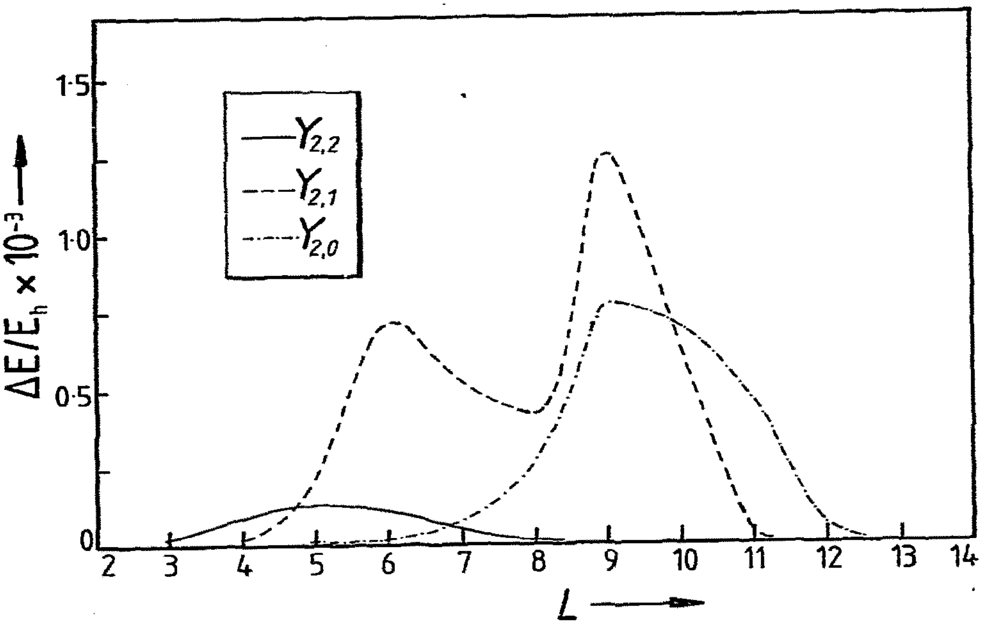

Fig. 1. Contributions to expression 9 for the inductive stabilization of ferrocene. The three curves give the separate contributions arising from excitation from $d_{xy}(Y_{22})$, $d_{xz}(Y_{21})$ and $d_{z^2}(Y_{20})$.

its metal—carbon distance is greater than that of ferrocene and this behaviour parallels that found for the inert gases.

If we combine the induction energy with that calculated in section 2 for the electrostatic energy we obtain a net stabilization of the eclipsed form of

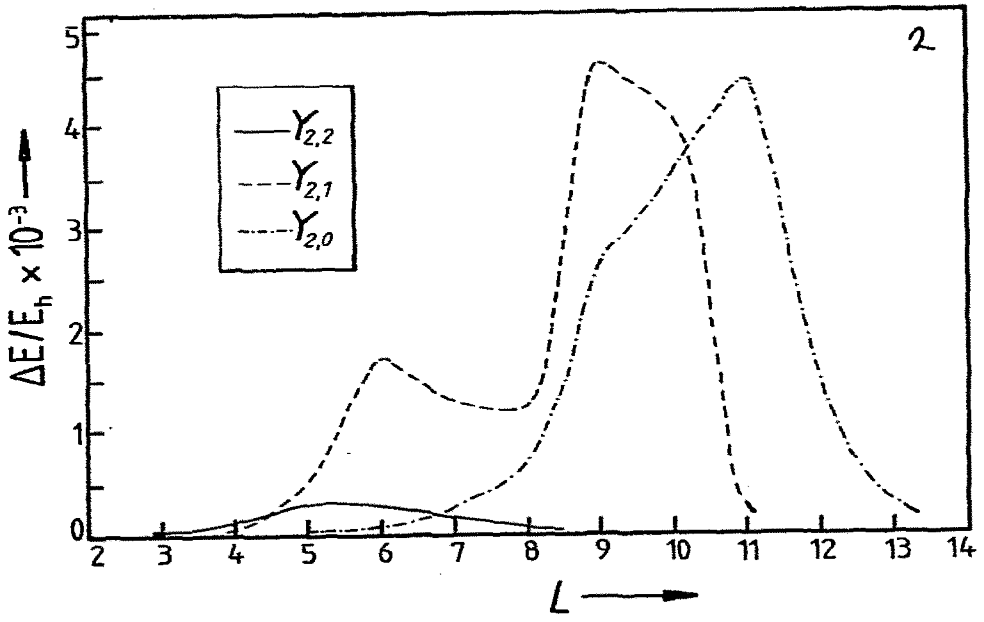

Fig. 2. As fig. 1 but for ruthenocene.

2.78 $kJmol^{-1}$ and 4.66 $kJmol^{-1}$ for ferrocene and ruthenocene respectively. The electron diffraction estimate for ferrocene is 3.8 ± 1.3 $kJmol^{-1}$ [8]. No experimental value is available for ruthenocene but because only the eclipsed structure has been detected the barrier is almost certainly larger than that of ferrocene.

Acknowledgement

We wish to thank Dr. M.G.B. Drew for helpful discussions on the X-ray data.

References

1 E.O. Fischer and W. Pfab, Z. Naturforsch. 137 (1952) 377.
2 P.F. Eiland and R. Pepinsky, J. Amer. Chem. Soc., 74 (1952) 4971.
3 J.D. Dunitz and L.E. Orgel, Nature, 171 (1953) 121.
4 J.D. Dunitz, L.E. Orgel and A. Rich, Acta. Cryst., 9 (1956) 373.
5 B.T.M. Willis, Acta. Cryst., 13 (1960) 1088.
6 B.T.M; Willis, AERE Report R3708, Harwell, Oxf.
7 R.K. Bohn and A. Haarland, J. Organometal. Chem., 5 (1966) 470.
8 A. Haarland and J.E. Nilsson, Acta. Chem. Scand., 22 (1968) 2653.
9 C.H. Holm and J.A. Ibers, J. Chem. Phys., 30 (1959) 885.
10 L.N. Mulay and A. Attala, J. Amer. Chem. Soc., 85 (1963) 702.
11 A.J. Campbell, C.A. Fyfe, D. Harold-Smith and K.R. Jeffrey, Mol. Cryst. Liq. Cryst., 36 (1976) 1.
12 P. Seiler and J.D. Dunitz, Acta. Cryst., B, 35 (1979) 1068, 2020.
13 F. Takusagawa and T.F. Koetzle, Acta. Cryst., B, 35 (1979) 1074.
14 G.L. Hardgrove and D.H. Templeton, Acta. Cryst., 12 (1959) 28.
15 L. Hedberg and K. Hedberg, J. Chem. Phys., 53 (1970) 1228.
16 A.K. Hedberg, L. Hedberg and K. Hedberg, J. Chem. Phys., 63 (1975) 1262.
17 J.N. Murrell in N.H. Masch (Ed.), Orbital Theories of Molecules and Solids, Oxford University Press, London, 1974, p. 374.
18 A.D. Buckingham in B. Pullman (Ed.), Intermolecular Interactions from Diatomics to Biopolymers, Wiley, New York, Ch. 1., 1978.
19 P. Claverie in B. Pullman (Ed.), Intermolecular Interactions from Diatomics to Biopolymers, Wiley, New York, Ch. 2., 1978.
20 K.F. Niebel and J.A. Venables, Proc. Roy. Soc. A, 336 (1974) 365.
21 S. Carter and J.N. Murrell. Molec. Phys., 32 (1976) 1269.
22 E. Clementi, At. Data and Nucl. Data Tables, 14 (1974) 177.
23 E.J. Baernards and P. Ros, Chem. Phys. Letters, 23 (1973) 391.
24 D.M. Brink and G.R. Satchler, Angular Momentum, Clarendon Press, Oxford, 1968.
25 C.C.J. Roothaan, J. Chem. Phys., 19 (1951) 1445.
26 Numerical Algorithms Group, N.A.G. Library Manual, Documents S14, (1974) 518.